FUEL DISTRIBUTION ESTIMATE VIA SPIN PERIOD TO PRECESSION PERIOD RATIO FOR THE ADVANCED COMPOSITION EXPLORER

Russell DeHart[(1)], **Eric Smith**[(2)], **and John Lakin**[(3)]

[(1)]*Honeywell Technology Solutions, Inc., 8800 Greenbelt Road, NASA Goddard Space Flight Center, Mail Code 444, Greenbelt, Maryland, 20771 USA, 301-286-2771, russell.r.dehart@nasa.gov*

[(2)] *Honeywell Technology Solutions, Inc., 8800 Greenbelt Road, NASA Goddard Space Flight Center, Mail Code 444, Greenbelt, Maryland, 20771 USA, 301-286-7394, eric.s.smith@nasa.gov*

[(3)] *Honeywell Technology Solutions, Inc., 8800 Greenbelt Road, NASA Goddard Space Flight Center, Mail Code 444, Greenbelt, Maryland, 20771 USA, 301-286-7071, john.v.lakin@nasa.gov*

Abstract: *The spin period to precession period ratio of a non-axisymmetric spin-stabilized spacecraft, the Advanced Composition Explorer (ACE), was used to estimate the remaining mass and distribution of fuel within its propulsion system. This analysis was undertaken once telemetry suggested that two of the four fuel tanks had no propellant remaining, contrary to pre-launch expectations of the propulsion system performance. Numerical integration of possible fuel distributions was used to calculate moments of inertia for the spinning spacecraft. A Fast Fourier Transform (FFT) of output from a dynamics simulation was employed to relate calculated moments of inertia to spin and precession periods. The resulting modeled ratios were compared to the actual spin period to precession period ratio derived from the effect of post-maneuver nutation angle on sun sensor measurements. A Monte Carlo search was performed to tune free parameters using the observed spin period to precession period ratio over the life of the mission. This novel analysis of spin and precession periods indicates that at the time of launch, propellant was distributed unevenly between the two pairs of fuel tanks, with one pair having approximately 20% more propellant than the other pair. Furthermore, it indicates the pair of the tanks with less fuel expelled all of its propellant by 2014 and that approximately 46 kg of propellant remains in the other two tanks, an amount that closely matches the operational fuel accounting estimate.*

Keywords: *Fuel Distribution, Moments of Inertia, Precession, Spin, Nutation.*

1. Introduction

ACE is a spin-stabilized spacecraft which orbits the Sun-Earth L1 libration point. Four blow-down fuel tanks are onboard the spacecraft, split into two pairs, pair A and pair B. The propulsion system performed nominally for the first 16 years of the mission. In September 2013 the B1 tank began to report increased temperatures. Subsequently, B1 and B2 tank temperatures increased by 5° C and maneuvers began to periodically underperform by as much as 50% in 2014. It is believed that these performance issues were caused by pressurant escaping into the fuel lines as two of the four onboard fuel tanks ran dry.

The fuel lines from all four tanks are interconnected; the pressurant lines, on the other hand, only connect tanks in a given pair. Sun sensor data is used to determine if a fuel imbalance was

present at the time of launch and if the B tanks expended their fuel in 2014. The ideal gas law is applied, showing the ratio of pressurant in one pair of tanks to that in the other pair, V_{N2_BtoA}, is constant while fuel remains in all tanks and that—given a small initial imbalance in fuel mass but equal at pressure—one pair of tanks could run dry significantly earlier than the other.

A finite element model generates spacecraft moments of inertia over the past 13 years. An FFT model using sun sensor data translates the history of moments of inertia into a history of predicted spin period to precession period ratios. The predicted ratios are compared to the observed ratios and the coefficient of determination, R^2, is calculated to determine the degree of fit. Trials with $R^2 \geq 0.988$ were collected as 'successful' trials. A 12,000,000-trial Monte Carlo search contained 175 successful trials. For all successful trials, V_{N2_BtoA} is contained in [1.531, 1.706], indicating that the fuel was unevenly distributed through the life of the mission and that the B tanks became empty in 2014. A second, finer Monte Carlo search is employed to provide best estimates of the fuel distribution, fitting uncertain parameters as necessary.

2. Background

2.1. Study Motivation

The Advanced Composition Explorer (ACE) is a spin-stabilized spacecraft that was launched on August 25, 1997. ACE orbits the Sun-Earth L1 libration point and provides near-real-time continuous coverage of solar wind parameters and solar energetic particle intensities. ACE performs attitude, orbit, and spin maneuvers using hydrazine thrusters. On average, ACE performs one maneuver per week. Four blow-down fuel tanks are onboard the spacecraft, split into two pairs (pair A and pair B). The propulsion system performed nominally for the first 16 years of the mission.

In September 2013 a small (0.01%) but unexplained increase in the spacecraft spin rate occurred. Also in September, the B1 tank began to report increased temperatures, as Fig. 1 illustrates.

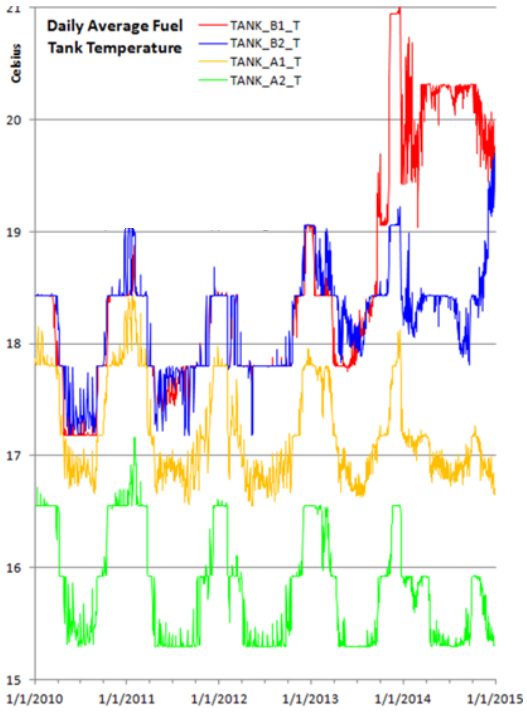

Figure 1. Daily average fuel tank temperature from telemetry

Figure 1 also shows the B1 tank temperature continued to increase to the point where in December 2013 the tank heaters—which had always been on for the length of the mission—began cycling on and off, causing the B1 tank temperature data to be less static. At this point, the mission began investigating a tank thermistor anomaly.

However in May 2014, maneuvers began to periodically underperform by 10 – 20%. A retrospective investigation of the earlier increased temperatures and the response of tank B1 to heater cycling as provided by Fig. 2 suggested tank B1 may be nearly devoid of fuel. This was initially met with some skepticism because the spacecraft propulsion system Critical Design Review (CDR) was interpreted at the time as implying the fuel should remain balanced onboard [1].

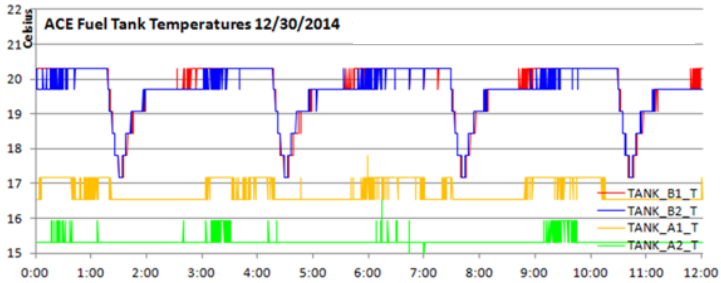

Figure 2. Tank temperatures during heater cycling

In November 2014, tank B2 began reporting increased temperatures and by December 2014 was reporting temperature data similar to tank B1. The spacecraft design is such that all four tank heaters are either on or off. Thus, the temperature responses shown in Fig. 2 illustrate that both

tanks in the B pair are acting in a manner consistent with having little to no fuel to act as a heat sink. Finally, in February 2015, maneuvers began to periodically underperform by as much as 50%.

2.2. Spacecraft Layout

The ACE propulsion system utilizes gaseous nitrogen to act as a pressurant in the blow-down hydrazine tanks. Fig. 3 is an illustration of the tanks, with the A-pair being the ones more closely aligned with the spacecraft body coordinate system (BCS) y axis. The system uses conispherical tanks, with the spacecraft spin forcing the fuel radially outward toward the tank nozzle.

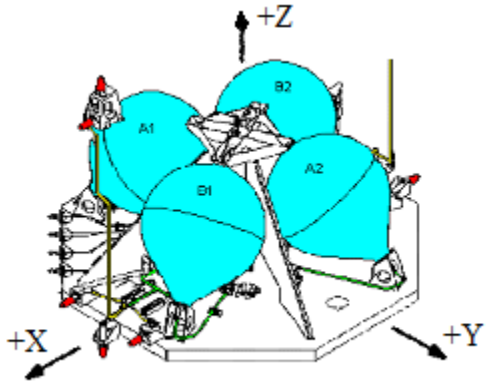

Figure 3. Fuel tank configuration and BCS axes

The fuel lines from all four tanks are interconnected. The pressurant lines, on the other hand, only connect tanks in a given pair, as is illustrated in the functional schematic provided in Fig. 4 [2]. This arrangement allows one pair of tanks to have a different amount of pressurant than the other. A difference in the amount of pressurant obscures imbalances in fuel. While the four fuel tanks may report equal pressures, this does not equate to equal fuel masses; rather, it simply means more pressurant is present in the tanks with less fuel. Had both the fuel and pressurant lines been interconnected, the fuel would be equally divided if all pressures were equal.

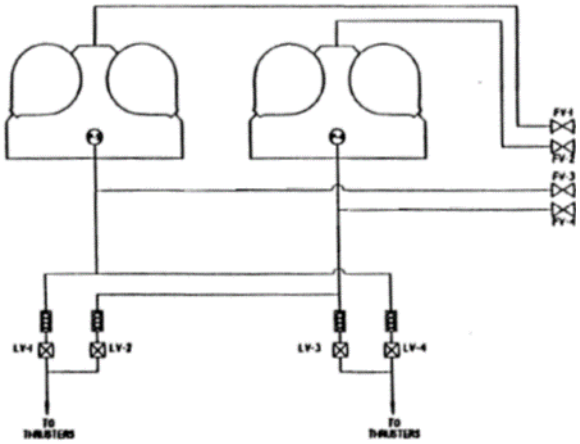

Figure 4. Fuel pressurant lines functional schematic

Once all fuel has been expelled from a pair of tanks and the corresponding fuel lines, pressurant escapes from the thrusters, causing marked underperformance. Since the fuel lines are interconnected, once a sufficient pressure difference exists between the two pairs of tanks, fuel from one pair can migrate to the empty fuel tanks and/or fuel lines. Once that fuel is expended, the cycle repeats itself. Hence, the design of the propulsion system allows for one pair of tanks to become empty, which then can cause periodic maneuver underperformance. This study uses attitude telemetry to determine if this is the cause of the telemetry and maneuver performance exhibited by ACE.

Both star scanner and sun sensor telemetry are available from the ACE attitude control system. The sun sensor data is provided more frequently, though. The spin period is determined by the time between sun pulses. A sun pulse is generated by the sun sensor once per spin when the sensor's X-axis crosses zero. The sun pulse timing accuracy is approximately 0.7 ms. On the other hand, the star scanner reports 4 stars every 64 s; for 20 minutes after each maneuver, 10 stars are reported every 16 s. Fine time resolution is needed in this study; consequently, sun sensor data is used and not star scanner data. Figure 5 provides diagrams showing the locations of the sun sensors, star scanner, thrusters.

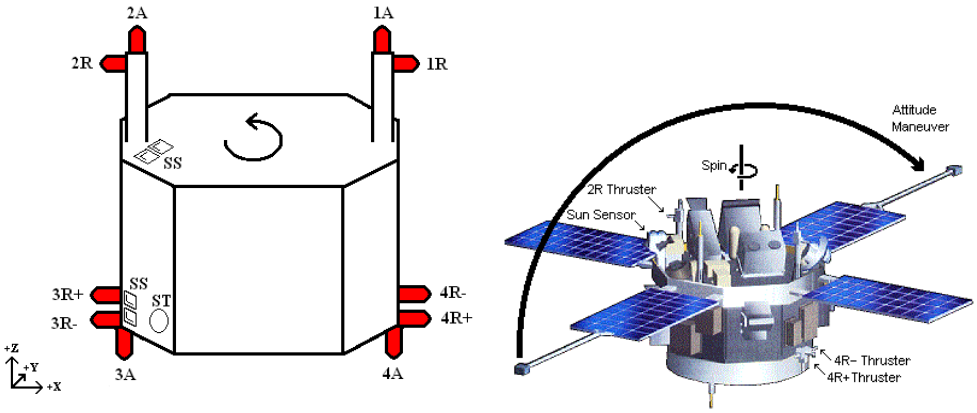

Figure 5. Locations of sun sensors (SS), star scanner (ST), and thrusters

3. Methodology

In order to minimize precession induced by maneuver thruster pulses, engineers designed ACE to have a spin period to precession period ratio, $P_{s:p}$, of 3:2, with a nominal spin period of 12 s. In doing so, the perturbations induced by each thruster pulse act against the system precession and nutation [3]. Equation 1 relates the design principal moments of inertia to the spin period to precession period ratio.

$$\frac{T_{spin}}{T_{precession}} \cong \frac{I_{spin}}{I_{transverse}} \tag{1}$$

The ratio $P_{s:p}$ can be determined using ACE sun sensor data after a maneuver. The induced precession of the spacecraft causes the sun sensor pulses to occur alternately earlier then later

than the 12-second nominal period, with a magnitude dependent on the nutation angle. Plotting the variability of the time between sun pulses yields results like those shown in Fig. 6.

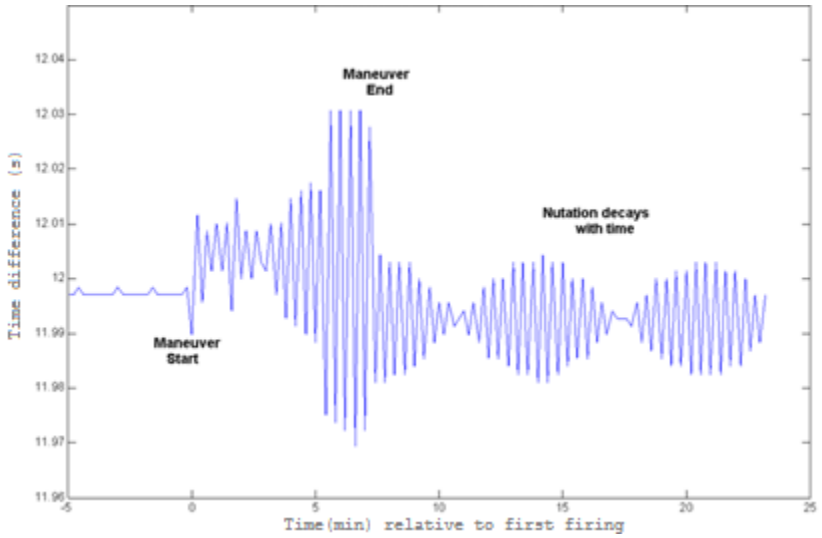

Figure 6. Time between sun sensor sun pulses after maneuver on 2014/133

The beat-like pattern shown in Fig. 6 occurs after each maneuver and is due to the stroboscopic effect. The period between 'beats' is dependent on the spacecraft spin and precession periods. As Fig. 6 illustrates, the beats observed after the maneuvers have periods of approximately 6 minutes. This period, along with the spin period as measured by sun pulse timing, can be used to measure $P_{s:p}$, using Eq. 2.

$$\frac{T_{spin}}{T_{precession}} = \frac{3}{2} - \frac{T_{spin}}{2 \times T_{beat}} \tag{2}$$

Figure 7 provides the history of this ratio from October 2001 to January 2015, calculated using Equation 2. When this ratio is plotted against estimated fuel remaining, a very strong linear trend is observed. The ratio becomes nearly constant when approximately 51 kg of fuel remain; this corresponds to the fuel estimate in August 2013, immediately before anomalous propulsion telemetry began to be reported. The estimated fuel is from a bookkeeping method, such as described in [4], and ±3 kg error bars are provided, reflecting the uncertainty reported from the pre-launch blow-down curve. These uncertainty bounds likely overstate the actual uncertainty and represent approximately 15 months' worth of fuel usage.

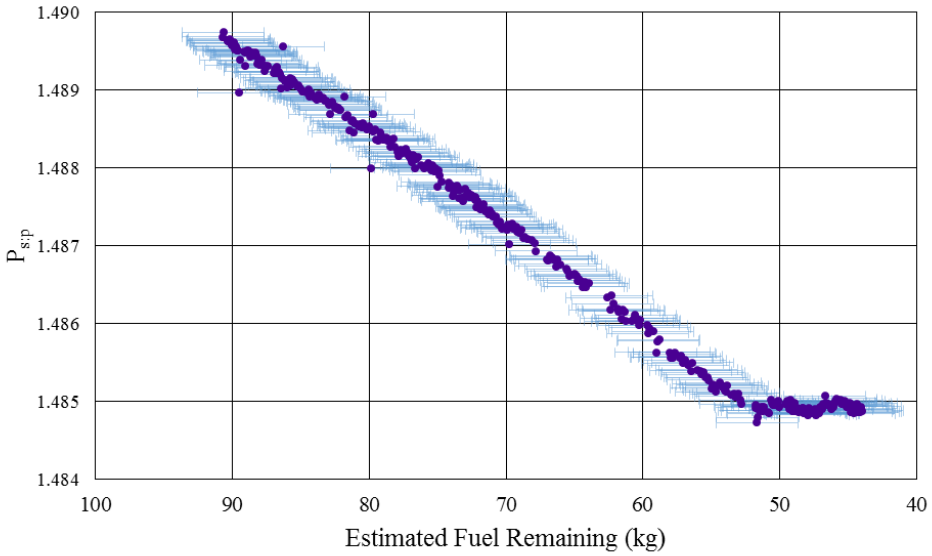

Figure 7. History of measured $P_{s:p}$, with mass uncertainty bars

A model of the spacecraft which determines the moments of inertia for a given fuel amount and distribution can produce an estimate of $P_{s:p}$ using Equation 1. The results can then be compared to the observed ratio values obtained using Equation 2. When the modeled fuel distribution is very close to that actually onboard for a given fuel mass, the modeled and observed $P_{s:p}$ values should agree within some small tolerance.

The value of the period ratio decreases only by 0.5% during the past 13 years, though. While Equation 1 provides an approximate relationship between the spacecraft moments of inertia and $P_{s:p}$, simulation runs indicated the approximation was not accurate enough for usage in this study. Consequently, this paper uses a torque free motion simulation to determine $P_{s:p}$ as a function of moments of inertia.

First, a finite element model is used to calculate the moments of inertia of the distributed fuel mass; these are then added to the documented dry moments of inertia to determine the spacecraft moments of inertia for a given fuel mass and distribution. Next, a numeric model of Euler's equations for torque-free motion and a fast Fourier transform (FFT) are used to generate a look-up table of $P_{s:p}$ values for given triplets of principal moments of inertia. The ideal gas law is used to determine the fuel distribution during the course of the mission for a given pre-launch fuel distribution. Finally, a Monte Carlo analysis is performed to determine what initial distribution of fuel generates period ratios that most closely resemble observed data, taking into account uncertainty in quantities such as the dry moments of inertia and tank nozzle locations.

The next sections of this paper provide additional model details. But the overarching goals of this study are to use these models to determine the fuel balance onboard and to determine if the B tanks became empty in late 2014. A secondary goal of this study is to use a Monte Carlo search to estimate the dry moments of inertia and the tank nozzle locations more accurately than documented values available to the mission. A second, finer Monte Carlo search is employed to provide best estimates of the fuel distribution, fitting uncertain parameters as necessary

4. Model Specifics

4.1. Fuel Tank Finite Element Model

The fuel in each tank is modeled using a 60 x 60 x 60-element grid. The location and geometry of the fuel tanks are provided by mechanical drawings available in the ACE propulsion subsystem critical design review (CDR). The drawings are not complete and visual inspection was used to estimate the fuel tank nozzle locations. The initial fuel mass and the dry mass properties are taken from the ACE pre-ship review [5]. Numeric integration of the finite element model is used to determine the fuel—and hence the overall—moments of inertia.

Propellant residing in the fuel lines is neglected. Slosh is also neglected, along with any other phenomena that would deform the propellant/pressurant interface. Hence, the fuel in each tank is modelled as a slug pinned against the outermost surface of the conispherical tank with the propellant/pressurant interface being parallel to the spacecraft spin axis. Additionally, the hydrazine density is treated as a constant value of 1.08 g/cm^3.

Due to the shared fuel and pressurant lines between the two tanks in a pair, each tank in a pair is treated identically in terms of the amount of pressurant and propellant present. In subsequent equations, each pair of tanks is treated as one unit.

Until 2013, pressure readings from the A tanks and B tanks matched within 1 least significant bit. Temperature readings also agreed well, and even after 2013, temperature differences were at most 5 K. Consequently, when modelling the nitrogen pressurant in the A and B tanks, the pressures and temperatures are treated as being equal. Since nitrogen behaves as an ideal gas at the temperatures and pressures observed in the tanks, the ideal gas law can be applied and simplifies to that shown in Equation 3, where *n* is the number of moles of nitrogen pressurant and *V* is the volume of the pressurant.

$$\frac{n_{B\ tanks}}{n_{A\ tanks}} \approx \frac{V_{Btanks\_pressurant}}{V_{Atanks\_pressurant}} \tag{3}$$

Since the pressurant is in a closed system—at least until nitrogen begins to escape due to little fuel remaining—the number of moles of nitrogen in the A and B tanks remains constant. Thus, the ratio of the nitrogen volume in the B tanks to the A tanks at the time of launch remains essentially constant through the course of the mission. Equation 4 shows the definition of a variable *nitrogen volume ratio, B to A, (V_{N2_BtoA}).*

$$V_{N2\_BtoA} \equiv \frac{V_{Btanks\_pressurant}}{V_{Atanks\_pressurant}} \approx constant \tag{4}$$

Using the total fuel mass and the density of hydrazine, the total hydrazine volume can be easily computed. The remaining tank volume, by definition, must be occupied by the nitrogen pressurant. The ratio V_{N2_BtoA} is then used to determine the volume of pressurant in the A tanks and in the B tanks. Equation 5 describes how to calculate the volume of the pressurant in the A

tanks; the volume of pressurant in the B tanks can be determined by applying the ratio V_{N2_BtoA}. The distribution of the fuel between the A tanks and B tanks follows directly from this, for the tank volume not consisting of pressurant consists of fuel.

$$V_{Atanks\_pressurant} = \frac{(V_{tanks\_total} - \frac{m_{hydrazine}}{\rho_{hydrazine}})}{(1+V_{N2_{BtoA}})} \tag{5}$$

The moment of inertia for a single tank over a range of fuel levels, from empty to full, is calculated in advance of the Monte Carlo runs and used as a lookup table with an independent cubic interpolation for each element of the inertia matrix. Since all 4 tanks are identically shaped, the same lookup can be used. This lookup table allows the determination of the tanks' moments of inertia for a given total fuel mass and a given value of V_{N2_BtoA}. Lastly, the result for each tank is rotated, translated via the parallel axis theorem, and added to the dry spacecraft moment of inertia to obtain the overall moments of inertia.

4.2. Fast Fourier transform model for $P_{s:p}$

Equations 6 – 8, Euler's equations for torque-free motion, are used to solve for the motion of the spacecraft following a perturbation that would generate precession. A typical spin rate is applied about the primary body axis and a smaller spin rate is applied about one of the transverse axes to offset the angular momentum by a typical post-maneuver nutation angle at the start of the propagation. Equations 9 & 10 are used to track a 3-1-3 Euler angle state (spin-nutation-precession, ψ-θ-φ) to determine the inertial orientation of the body axes [7]. In this way the asymmetry of the transverse moments of inertia is correctly taken into account. Fuel slosh and external torques are neglected.

$$I_1\dot{\omega}_1 = (I_2 - I_3)\omega_2\omega_3 \tag{6}$$
$$I_2\dot{\omega}_2 = (I_3 - I_1)\omega_3\omega_1 \tag{7}$$
$$I_3\dot{\omega}_3 = (I_1 - I_2)\omega_1\omega_2 \tag{8}$$

$$\vec{b}_{inertial} = [R_3(\psi)R_1(\theta)R_3(\varphi)]^T\vec{b}_{BCS} \tag{9}$$

$$\begin{bmatrix}\dot{\varphi}\\ \dot{\theta}\\ \dot{\psi}\end{bmatrix} = \frac{1}{\sin(\theta)}\begin{bmatrix} sin(\psi) & cos(\psi) & 0\\ cos(\psi)sin(\theta) & -sin(\psi)sin(\theta) & 0\\ -sin(\psi)cos(\theta) & -cos(\psi)cos(\theta) & sin(\theta)\end{bmatrix}\begin{bmatrix}\omega_1\\ \omega_2\\ \omega_3\end{bmatrix} \tag{10}$$

Propagations used a Runge-Kutta method (Dormand-Prince 8(5, 3)), and an initial spin period of 12 s. Without loss of generality, here ω_3 is the spin rate about the BCS Z axis and ω_1 and ω_2 are rotations about the BCS X and Y axis, respectively. An initial angular velocity about ω_1 similar to that seen immediately after maneuvers is also used. All other angular velocity and accelerations are 0 initially. Figure 8 illustrates the layout of these axes.

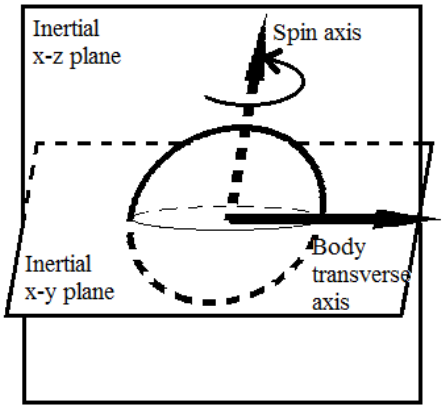

Figure 8. Simplified diagram of body and inertial frames used in FFT model

A fast Fourier transform was performed on the inertial x and z components of the BCS X axis to determine the spin and precession periods, respectively. Long propagations (8,192 s = 2^{13} s) were used to obtain high-precision frequency measurements from the FFT; the resulting measurement precision of $P_{s:p}$ is 0.0016%, including the effects of interpolation. Figures 9 & 10 provide sample output, showing the strong frequency responses that correspond to the spin and precession frequencies (from which the periods follow).

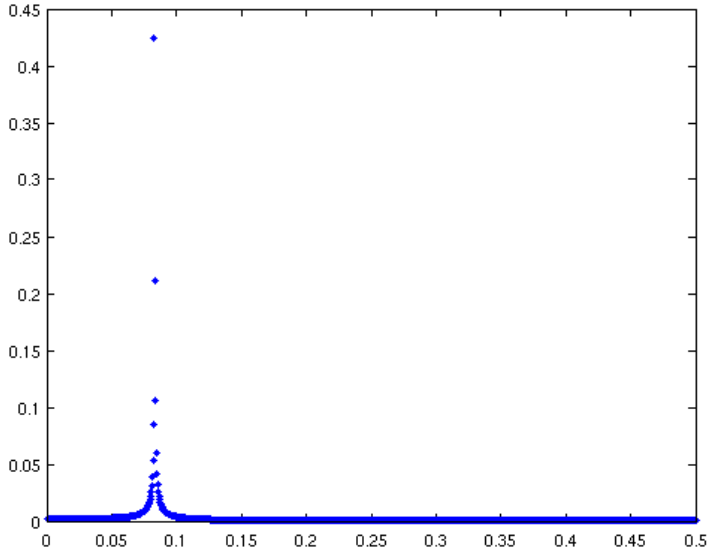

Figure 9. Sample FFT frequency response for spin (f = 0.08350 Hz, T = 11.98 s)

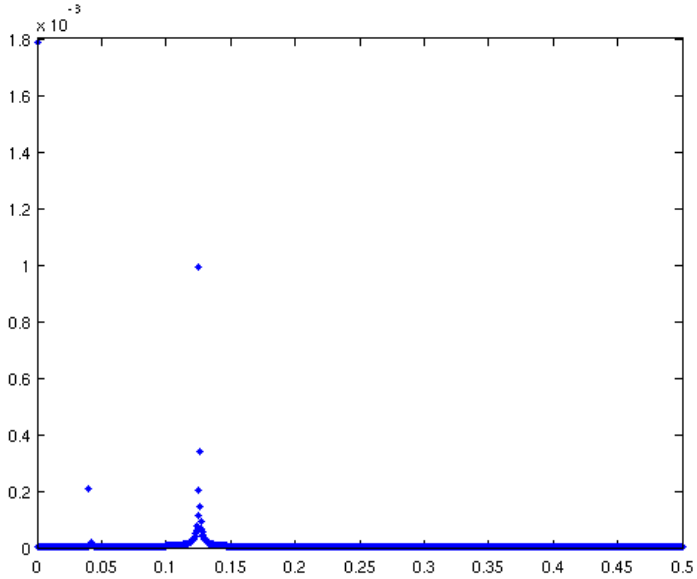

Figure 10. Sample FFT frequency response for precession (f = 0.1125 Hz, T = 7.968 s), also showing response for nutation (f = 0.04102 Hz, T = 23.38 s)

In order to decrease simulation run time, principal moments of inertia were selected combinatorially from a 1-kgm^2 grid of values that spanned all moments of inertia observed in this study. The results were used as a lookup table, with tri-cubic interpolation, for the Monte Carlo runs. Once the moments of inertia are determined using the first lookup table, this next lookup table is used to supply the corresponding $P_{s:p}$, rather than having to run a time-consuming propagation and FFT each time. The time savings are necessary for the Monte Carlo analysis performed in this study.

4.3. Model Summary

Figure 11 supplies an overview of the complete ACE model used in this study. Estimated fuel masses and the corresponding measured spin-to-precession ratios over the past 13 years have been compiled. Each total fuel mass is distributed to the 4 tanks using a selected value of V_{N2_BtoA}. The mass of each tank is used to lookup the associated moment of inertia matrix. The matrices for all four tanks are combined into a total spacecraft inertia matrix, which is then diagonalized to determine the principal moments of inertia. Those principal moments of inertia are used to lookup the spin-to-precession ratio that corresponds to that particular total fuel mass given the chosen V_{N2_BtoA}. Finally, the predicted ratios are compared to the observed ratios and the coefficient of determination, R^2, is calculated to determine the degree of fit.

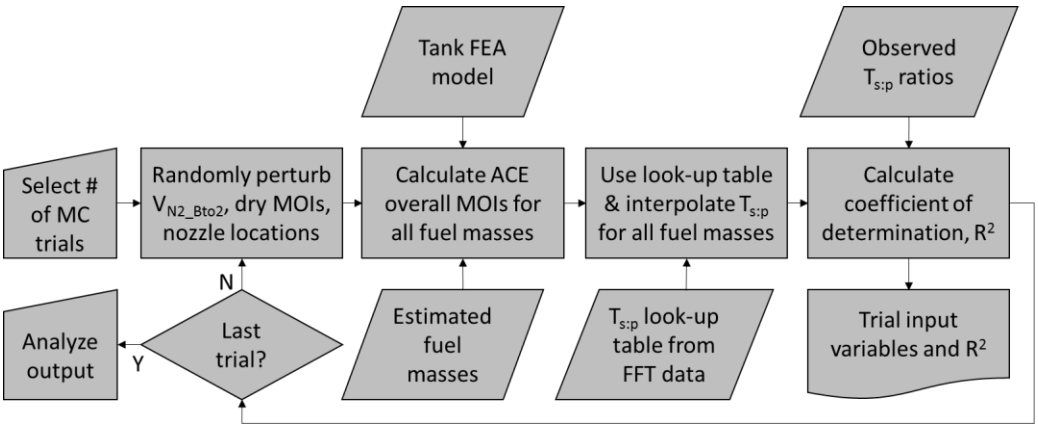

Figure 11. ACE model overview

4.4. Monte Carlo Summary

Two Monte Carlo analyses are performed in this study. First, the value of V_{N2_BtoA} is allowed to vary over a wide range and uncertainty values are assigned to dry moments of inertia and the tank locations. A wide range of V_{N2_BtoA} is initially used to demonstrate that the only values which match observations also cause the B tanks to run dry in 2014. After identifying the range of V_{N2_BtoA} that is most consistent with observations, a second, finer Monte Carlo search is performed. This search is executed to identify sets of values for V_{N2_BtoA}, dry moments of inertia, and tank locations that generate $P_{s:p}$ values that most closely match observations.

4.5. Selection of Monte Carlo Perturbations

The ACE CDR states that the launch configuration moments of inertia have an accuracy of 1.5%, without stating the confidence level. For the purposes of this study, all dry moments of inertia are allowed to vary by +/- 4.5%. The locations of the fuel tank nozzles were identified using the mechanical drawings presented in the ACE propulsion portion of the ACE CDR. However, these drawings provided only estimates of the nozzle locations within ½ inch of a nominal location. In order to account for uncertainty in this estimate, and uncertainty in the difference between the design placement and the actual placement, the tank nozzle coordinates are allowed to vary by +/- 1 inch. Lastly, those tanks nozzle coordinates were documented in the propulsion coordinate system (PCS). This system is aligned with the BCS, but the origin is offset ($Z_{BCSoffset}$) in the +Z direction from the BCS. In order to write the tank coordinates in the BCS frame, $Z_{BCSoffset}$ was first determined. Hardware for which coordinates could be found in both the BCS and PCS frames were used to determine this offset. Again, though, to allow for uncertainty in actual hardware placement—and to be consistent with the uncertainties mentioned thus far—$Z_{BCSoffset}$ is also allowed to vary by +/- 1 inch. All uncertain parameters were sampled from uniform distributions.

For the first Monte Carlo analysis, V_{N2_BtoA} was sampled from a uniform distribution spanning 0.5 – 2.5. Table 1 summarizes the nominal values and uncertainty bounds for the perturbed variables. For the second Monte Carlo analysis, inputs were sampled from uniform distributions

spanning the ranges of values that generated $P_{s:p}$ values that most closely match observations in the first analysis.

Table 1. Sample Space used in First Monte Carlo Analysis

Quantity	Nominal Value	Sample Space
V_{N2_BtoA}	1.0*	U[0.5,2.5]
$I_{xx,dry}$	324.44 kgm^2	U[nominal – 4.5%, nominal + 4.5%]
$I_{yy,dry}$	249.59 kgm^2	U[nominal – 4.5%, nominal + 4.5%]
$I_{zz,dry}$	436.16 kgm^2	U[nominal – 4.5%, nominal + 4.5%]
$I_{xy,dry}$	-0.14 kgm^2	U[nominal – 4.5%, nominal + 4.5%]
$I_{xz,dry}$	0.03 kgm^2	U[nominal – 4.5%, nominal + 4.5%]
$I_{yz,dry}$	0.01 kgm^2	U[nominal – 4.5%, nominal + 4.5%]
$Z_{BCSoffset}$	0.280 m	U[nominal – 1”, nominal + 1”]
A1 nozzle location	(-0.569, -0.236, 0.109) m	x,y,z ϵ U[nominal – 1”, nominal + 1”]
A2 nozzle location	(0.569, 0.236, 0.109) m	x,y,z ϵ U[nominal – 1”, nominal + 1”]
B1 nozzle location	(0.236, -0.569, 0.109) m	x,y,z ϵ U[nominal – 1”, nominal + 1”]
B2 nozzle location	(-0.236, 0.569, 0.109) m	x,y,z ϵ U[nominal – 1”, nominal + 1”]

* 1.0 indicates balanced fuel tanks, which before 2013 was believed to be the nominal state

5. Results

5.1. Initial Monte Carlo search results: Are the B tanks empty?

For each Monte Carlo trial, $P_{s:p}$ was calculated for each estimated fuel mass in the observed data. To compare each trial's history of ratios to the observed history of ratios over the past 13 years, the coefficient of determination, R^2, was calculated.

Initial Monte Carlo runs were executed and trials with large values of R^2 (> 0.9) were examined. Trials with $R^2 \geq 0.988$ were visually judged to have very close agreement between predicted and observed ratios. This lower bound is used to define when a trial is a 'success.'

A 12,000,000-trial Monte Carlo was performed and 175 successful trials were identified. For all successful trials, V_{N2_BtoA} is contained in [1.531, 1.706]. To indirectly measure the likelihood that some other region of the sample space would have yielded successful trials, a confidence interval was calculated. The actual population ratio of the space that yields a success to the entire sample space is p. The Monte Carlo analysis provides a sample estimate, p_N, of 1.46×10^{-5}. The Clopper-Pearson 95th percentile confidence limits for this binomial distribution are [1.25×10^{-5}, 1.69×10^{-5}]. Given the relative tightness of this range compared to the sample estimate, it is likely that the subspace in which V_{N2_BtoA} is contained within roughly [1.53, 1.71] is the only successful region in the full sample space.

To visualize the level of agreement obtained by the successful trials, Fig. 12 provides a plot of the predicted and observed $P_{s:p}$ for the most successful trial from the first Monte Carlo set, for which $R^2 = 0.998$.

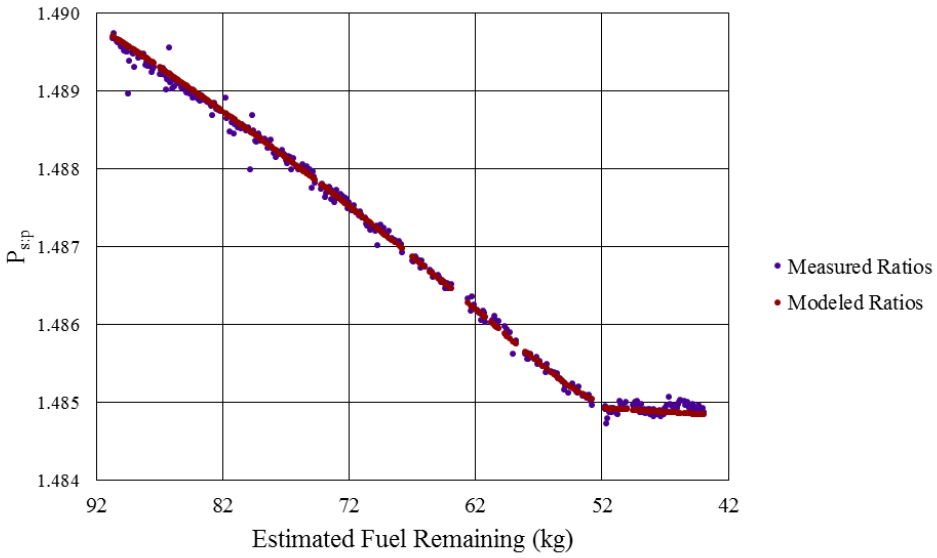

Figure 12. Modeled and measured $P_{s:p}$ for best result from the broad search

The range of V_{N2_BtoA} for the successful trials indicates the fuel was not evenly distributed among the tanks at the time of launch. Lending further credence to this finding, the 'elbow' present in the observed data corresponds to approximately one month before the B1 tank began reporting increased temperatures. In the modeled data, the appearance and location of the elbow was dictated solely by the value of V_{N2_BtoA}; moreover, the elbow occurs in the modeled data when one pair of tanks becomes dry. Hence, the presence of the elbow in the data strongly suggests the B1 tank became nearly devoid of fuel when increased temperatures began to be reported.

By contrast, trials in which the value of V_{N2_BtoA} was nearly 1.0 (i.e., the fuel is divided equally in the tanks and fuel currently remains in all tanks) do not perform well, particularly with respect to fitting observed data once B tank telemetry became anomalous. Figure 13 provides output from the trial with $V_{N2\_BtoA} \sim 1$ that reported the highest value of R^2 (V_{N2_BtoA} =1.002, R^2 = 0.978). The uncertainty values of the measured ratios originally shown in Fig. 7 are repeated here. The key feature in the observed history of $P_{s:p}$—the flattening of the ratio when approximately 51 kg of fuel remains—is missing from this trial and all other trials with $V_{N2\_BtoA} \sim 1$. While the uncertainties in the measured data allow for uncertainty in the slope of the linear trend of $P_{s:p}$ while more than 51 kg of fuel remains, they do not allow for that trend to continue past the elbow point. To further test the ability of balanced tanks to fit observed data, an additional Monte Carlo run of 4,000,000 trials was executed, with no trial surpassing the 'success' threshold for R^2. Thus, evenly distributed fuel at the time of launch is incompatible with observed data.

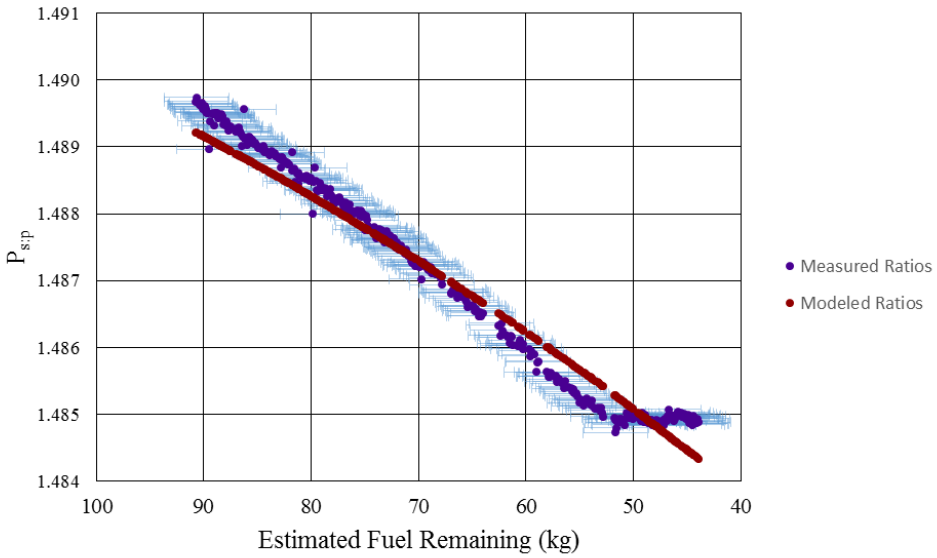

Figure 13. Modeled $P_{s:p}$ for best fitting trial with $V_{N2\_BtoA} \sim 1$ ($R^2 = 0.978$, $V_{N2\_BtoA} = 1.002$) as compared to measured history of $P_{s:p}$ with uncertainty bars

5.2. Refined Monte Carlo search results: Identifying actual spacecraft configuration

In the set of successful trials from the first Monte Carlo analysis, minimal correlations were present between all tank location input variables. Also, for those successful trials the coordinate values essentially spanned their sampled range. Hence, for the second Monte Carlo analysis, all input values related to tank locations were sampled in the same fashion as during the first analysis.

In the set of successful trials from the first Monte Carlo analysis, values of $I_{xx,dry}$ and $I_{yy,dry}$ also spanned their sample space and showed negligible correlation to each other ($r = -0.056$). From that set of successful trials $I_{zz,dry}$ did not span the sample space (instead spanned 416 – 448 kgm^2) and visually did not appear to be uniform in distribution. Tests using the sample second, third, and fourth moments were not able to identify the distribution of $I_{zz,dry}$, though [6]. Although $I_{xx,dry}$ and $I_{yy,dry}$ exhibited strong correlation with $I_{zz,dry}$ ($r = 0.869$ and 0.445, respectively), the lack of a distribution to use for $I_{zz,dry}$ is an impediment to using the correlation between the dry moments of inertia when sampling $I_{xx,dry}$, $I_{yy,dry}$, and $I_{zz,dry}$ for the second Monte Carlo analysis. Consequently, $I_{xx,dry}$ and $I_{yy,dry}$ were sampled uniformly in the same fashion as the first analysis and $I_{zz,dry}$ was sampled uniformly from [416, 448] kgm^2.

The second analysis used 4,000,000 trials. The value of R^2 is again used to measure the degree of fit between the predicted $P_{s:p}$ and observed $P_{s:p}$ values. The 0.01% of the trials with the highest value of R^2 were collected and represent the *best fit set*. Table 2 presents the median, $\tilde{x}$, and sample standard deviation, s, for the input variables from the best fit set, along with the nominal values. Figure 14 provides the output from the trial with the highest value of R^2 ($R^2 = 0.998$).

Table 2. Best Fit Set Estimates of Actual Spacecraft Configuration, Compared To Nominal Values

Quantity	Best fit set $\tilde{x}$	Best fit set s	Nominal value
V_{N2_BtoA}	1.621	0.027	1.0*
$I_{xx,dry}$	327.89 kgm^2	7.70 kgm^2	324.44 kgm^2
$I_{yy,dry}$	246.47 kgm^2	6.32 kgm^2	249.59 kgm^2
$I_{zz,dry}$	431.04 kgm^2	7.58 kgm^2	436.16 kgm^2
$Z_{BCSoffset}$	0.292 m	0.011 m	0.280 m
A1 nozzle location	(-0.576, -0.238, 0.113) m	s_x=s_y =s_z = 0.014 m	(-0.569, -0.236, 0.109) m
A2 nozzle location	(0.576, 0.236, 0.116) m	s_x=s_y =s_z = 0.014 m	(0.569, 0.236, 0.109) m
B1 nozzle location	(0.239, -0.567, 0.108) m	s_x=s_y =s_z = 0.014 m	(0.236, -0.569, 0.109) m
B2 nozzle location	(-0.236, 0.569, 0.110) m	s_x=s_y =s_z = 0.015 m	(-0.236, 0.569, 0.109) m

* 1.0 indicates balanced fuel tanks, which before 2013 was believed to be the nominal state

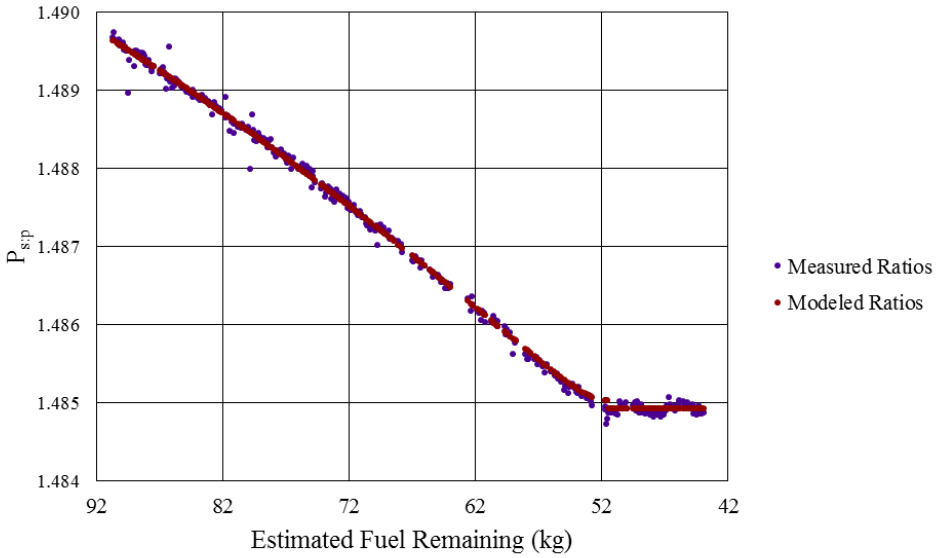

Figure 14. Modeled and observed $P_{s:p}$ for best result from refined search

All nominal values are within one sample standard deviation of the best fit set median values, except for V_{N2_BtoA}, which is restricted to a tight range that does not include 1.0 ($\tilde{x}$ = 1.621, s = 0.027). Consequently, results from this study's model are consistent with the documented spacecraft configuration with one exception. The pressurant—and hence the propellant—was unevenly distributed onboard at launch. The median value of 1.621 for V_{N2_BtoA} corresponds to a fuel distribution of 55.1%/44.9% between the A and B tanks, respectively, at the time of launch.

6. Conclusion

Based on the results of this study, it is very likely that at the time of launch the fuel was not evenly distributed among the four fuel tanks. The pressurant line design and unequal loading of pressurant hid this discrepancy until anomalous propulsion system telemetry began in 2013. All Monte Carlo trials that match ($R^2 \geq 0.988$) observed spin period to precession period ratios have the B tanks becoming empty in 2014. All spacecraft configuration values perturbed in the Monte

Carlo searches performed in this study remain, for successful cases, within one sample standard deviation of pre-launch documented values with one exception—the fuel distribution. The Monte Carlo search estimates 1.621 times as much nitrogen existed in the B tanks than in the A tanks at the time of launch. This corresponds to 55.1% of the fuel being in the A tanks and 44.9% being in the B tanks at launch. Based on the findings of this study, the ACE mission closed the B-side latch valves on March 17, 2015 to prevent pressurant from escaping through the thrusters which thereby causes maneuver underperformance. Since doing so, maneuvers have returned to historically nominal performance.

7. References

[1] Swink, D. G. et al., "Advanced Composition Explorer Critical Design Review," Olin Aerospace Company, 94-H-1973, Redmond, WA, May 1994.

[2] Margolies, D. et al., "Advanced Composition Explorer Mission Critical Design Review," NASA, Nov. 1994.

[3] Woodard, M. and Baker, D. "Optimal attitude maneuver execution for the Advanced Composition Explorer (ACE) mission." Proceedings Flight Mechanics/Estimation Theory Symposium 1995. Greenbelt, MD, USA, 1995.

[4] Yendler, B. "Review of Propellant Gauging Methods." Proceedings 44th AIAA Aerospace Sciences Meeting and Exhibit. Reno, Nevada, USA, 2006.

[5] Chiu, M. C. et al., "Advanced Composition Explorer Pre-Ship Review," The Johns Hopkins University Applied Physics Laboratory, Laurel, MD, June 1997.

[6] Hahn, G. J. and Shapiro, S. S., *Statistical models in engineering*, Wiley, New York, 1994.

[7] Wie, Bong, *Space Vehicle Dynamics and Control Second Edition*, AIAA, 2008.